Supporting Information

Letellier et al. 10.1073/pnas.0902820106

SI Results

After 25 days in vitro (25 DIV), we found that the central features of the cerebellar system were present, but with a modified tridimensional organization (1). The principal cellular elements displayed a pseudolobular organization and were arranged in layers reminiscent of lamination in vivo (Fig. S1 *B*, *D–G*).

In most cases, CaBP immunopositive PCs were arranged in a pseudomonolayer (Fig. S1 *B*, *E–G*). They were polarized and usually orientated their dendritic tree toward the top of the explant (Fig. S1 *B*, *E–G*). Many Pax6-positive granule cells (GCs) were present; they were usually restricted either below or sometimes above the PC layer (Fig. S1*E*). Parvalbumin-positive interneurons were also found at the level of the PC layer and sometimes below (Fig. S1*F*). GFAP-positive glial cells were found in the lower part of the explant, extending processes throughout the entire thickness of the explants and establishing close contacts with PCs (Fig. S1*G*).

We also verified whether the pattern of excitatory synapses onto mature PCs from explants at 25 DIV (corresponding chronologically to age P19) was the same as in vivo. PF terminals from GCs and CF terminals from olivary neurons were labeled with VGLUT1 and VGLUT2 antibodies, respectively. Because VGLUT2 is also expressed by mossy fibers (MF) and transiently by PFs during development in vivo (2), CF morphology was also analyzed with anterograde tracing (Fig. S2 *A1*, *A2*, *A4*, *B4*, and *C*).

Confocal images showed that all PCs (28 cells, 5 explants) innervated by VGLUT2-positive terminals from an anterograde-traced CF were contacted primarily on their soma and, when visible, on their dendritic trunk (see Fig. S2 *A1–A4*, *C*, and *E*). In contrast, less than 5% of PC cell bodies (1 cell of 21, 3 explants) were contacted by VGLUT1-immunopositive PF terminals, but all visible dendrites were contacted by PFs terminals on their spines (Fig. S2 *B1–B4*, *D*, and *E*). Thus, a subcellular segregation between PFs and CFs exists in explants, as in vivo (Fig. S2*H*).

SI Methods

Animals. Pregnant Swiss mice were purchased from Janvier and were used for culturing explants and/or cerebellar plates at E14. Transgenic mice expressing green fluorescent protein (GFP) under the control of the chicken β-actin promoter (actin-GFP) have been described previously (3) and were obtained from Dr. I. Dusart (Université P. et M. Curie, Paris); they were used for coculture experiments (see below). Animal housing and all procedures were performed under the guidelines established by le Comité National d'Ethique pour les Sciences de la Vie et de la Santé, which are in accordance with the European Communities Council Directive (86/609/EEC).

Organotypic Cultures. Cultures of hindbrain explants or cerebellar plates were performed as described previously (1) (Fig. S1*A*) by using Swiss or actin-GFP mice at embryonic day 14 (E14). E0 was the mating day. Briefly, the embryos' heads were put into ice-cold Gey's balanced salt solution (Eurobio) with 5 mg/mL glucose, and brains were quickly dissected out. The brain region between the tecto-cerebellar and medullo-spinal junctions (including the cerebellar anlage and the inferior olive nucleus) or cerebellar plates alone were isolated, and the meninges were removed. Explants were then transferred onto membranes of 30-mm Millipore culture insert plates (pore size 0.4 μm, Millicell CM; Millipore) in six-well plates with 1 mL/well of medium containing 50% basal medium with Earle's salts (Invitrogen), 25% Hank's Balance Salt Solution (Invitrogen), 25% horse serum (Invitrogen), 1 mM L-glutamine, and 5 mg/mL glucose at 35 °C in a humidified atmosphere with 5% CO_2. Zero days in vitro (DIV) was the culturing day. The medium was replaced every 2–3 days.

Cocultures. For coculture experiments, Swiss cerebellar plates were separated from the brainstem either before culturing at 0 DIV or at 21 DIV. Mature PCs from the cerebellar plates separated at 0 DIV were referred to as naive PCs (i.e., they have never experienced CF-innervation); mature PCs from those separated at 21 DIV were referred to as non-naive PCs (they have been CF-innervated). Mature PCs were then allowed to be (re)innervated by immature or mature CFs. In a first set of experiments, cerebellar plates at 21 DIV were placed in close contact with cerebellar plates from intact actin-GFP hindbrain explants at 21 DIV (isochronic cocultures; Fig. 2 *A* and *B*). In a second set of experiments cerebellar plates at 21 DIV were placed in close contact with embryonic actin-GFP brainstems at 0 DIV (heterochronic cocultures; Fig. 2 *C* and *D*).

Electrophysiology. Whole-cell patch-clamp recordings from PCs were performed as previously described for acute cerebellar slices (4). For voltage-clamp recordings, patch pipets were filled with a solution containing: 120 mM Cs-D-Gluconate, 13 mM biocytin, 10 mM HEPES, 10 mM BAPTA, 3 mM TEACl, 2 mM Na_2ATP, 2 mM MgATP, 0.2 mM NaGTP, pH 7.3, 290–300 mM mOsm. For current-clamp recordings, patch pipets were filled with a solution containing: 140 mM K-D-gluconate, 10 mM HEPES, 1 mM EGTA, 6 mM KCl, 0.1 mM $CaCl_2$, 5 mM $MgCl_2$, 4 mM NaATP, 0.4 mM NaGTP, pH 7.3, 290–300 mM mOsm. Explants were continuously perfused with a bath solution containing: 125 mM NaCl, 2.5 mM KCl, 1.25 mM NaH_2PO_4, 26 mM $NaHCO_3$, 2 mM $CaCl_2$, 1 mM $MgCl_2$, 25 mM glucose, and bubbled with 95% O_2 and 5% CO_2. Picrotoxin (100 μM) was added to block inhibitory currents. Series resistance was compensated (60–80%).

CF-EPSCs were elicited by stimulation with a saline-filled glass pipet in the area surrounding the PC. We distinguished CF-EPSCs from currents mediated by parallel fibers (PF-EPSCs) by their all-or-none character and by the demonstration of paired-pulse depression (5). To determine the number of CFs innervating a PC, we counted the number of discrete CF-EPSC steps that appeared when the intensity of stimulation was gradually increased or when the position of the stimulation electrode was changed.

Currents and potentials were recorded from PCs using either Axopatch 200A or 200B amplifiers (Axon Instruments). We used Acquis 1 and Elphy (Biologic) for data acquisition and analysis of EPSCs. sEPSCs, recorded at −80 mV, were detected and analyzed using MiniAnalysis (Synaptosoft). A detection threshold was set at −15 pA.

Following electrophysiological recordings, explants were fixed in 4% paraformaldehyde (PFA) in PB 0.1 M and processed for immunohistochemistry; the recorded (biocytin-filled) PCs were visualized after incubation with AF350-conjugated avidin (Invitrogen, Molecular Probes).

Anterograde Tracing. Under a dissecting microscope, a small volume (10–500 nL) of fluorodextran tracer (10% in PBS, dextran-FITC conjugate, 10,000 MW; Invitrogen, Molecular

Probes) was injected into the inferior olivary nucleus with a glass pipet to reveal olivary axons and their CF terminals. Explants injected at either 10 or 21 DIV were incubated for a further 4 days before fixing with 4% PFA in 0.1 M PBS and processing for immunohistochemistry.

Immunohistochemistry. For immunohistochemical visualization of glutamatergic terminals onto PCs, injected explants were fixed with 4% PFA at 14 DIV or 25 DIV and were subsequently incubated with a monoclonal mouse anti-CaBP antibody (1:5,000; Swant) in combination with either polyclonal guinea pig (GP) anti-vesicular glutamate transporter 1 (VGLUT1) or anti-VGLUT2 antibodies (1:3,000; Chemicon). After incubation with the primary antibodies, explants were incubated in a mixture of Cy3-conjugated donkey anti-GP (1:200; Jackson ImmunoResearch Laboratories) and Alexa Fluor 405-conjugated goat anti-mouse (1:100; Invitrogen, Molecular Probes) antibodies.

For visualization of contacts between mature PCs and actin-GFP fibers penetrating cerebellar plates in co-culturing experiments, explants were fixed and subsequently incubated with monoclonal mouse anti-CaBP (1:5,000; Swant) and Alexa Fluor 488-conjugated rabbit anti-GFP (1:200; Invitrogen, Molecular Probes) antibodies. Immunofluorescence for CaBP was visualized after incubation with Cy3-conjugated donkey anti-mouse antibody (1:200; Jackson ImmunoResearch Laboratories).

For immunohistochemical visualization of cerebellar cell populations, explants at 25 DIV were fixed with 4% PFA in 0.1 M PBS. After cryoprotection in 10% sucrose in 0.1 M PBS, they were included in 7.5% gelatin with 10% sucrose added and subsequently frozen in isopentane. Transverse cryostat sections (10 μm thick) were obtained for immunohistochemical analysis. Cryosections were incubated with monoclonal mouse or polyclonal rabbit anti-Calbindin D28K antibody (CaBP, 1:5,000; Swant) in combination with either polyclonal rabbit anti-Pax6 (1:1,000; Chemicon), polyclonal rabbit anti-parvalbumin (PV, 1:5,000; Swant) or monoclonal mouse anti-glial fibrillary acidic protein (GFAP, 1:100; Cell Signaling) antisera. Immunofluorescence was visualized after incubation with FITC-, AMCA-, or Cy3-conjugated species-specific secondary antibodies (1:200; Jackson ImmunoResearch Laboratories).

Finally, sections or explants were mounted in Mowiol (Calbiochem) and examined using either standard epifluorescence microscopy (Eclipse E800; Nikon) or an inverted confocal microscope (MI 6000; Leica). The Reconstruct Program (http://synapses.clm.utexas.edu/; ref. 6) was used to make three-dimensional reconstructions from confocal data stacks of PCs innervated by anterograde-traced CFs.

Data Analysis. The disparity between amplitudes from CFs-EPSCs recorded in a given PC at the same holding potential was calculated as described (7). The "Disparity Index" and the "Disparity Ratio" were calculated for each recorded PC.

Disparity Index = SD/M; SD is the standard deviation; $M = \sum A_i/N$; $(i = 1, 2, 3, \ldots, N; n \geq 2)$

Disparity Ratio = $(A_1/A_N + A_2/A_N + \ldots + A_N - 1/A_N)/(N - 1)$; $(i = 1, 2, 3, \ldots, N; n \geq 2)$

A_i is the EPSC amplitude for the CF_i, and N is the number of CF for a given PC.

Statistical Analysis. The Chi^2 test was used to compare percentages of PCs innervated by one or more CFs between experimental groups. For normally distributed data (normality determined with the D'Agostino-Pearson normality test), statistical differences were assessed using the two-tailed *t*-test or the one-way ANOVA followed by the Scheffé or the Bonferroni posthoc tests. The Mann-Whitney test was used when the criteria for normality were not met. In figures, statistical significance is indicated by *, for $0.05 < P < 0.01$; **, for $0.01 < P < 0.001$; and ***, for $P < 0.001$. Average data are expressed as mean ± SEM.

1. Chédotal A, Bloch-Gallego E, Sotelo C (1997) The embryonic cerebellum contains topographic cues that guide developing inferior olivary axons. *Development* 124:861–870.
2. Miyazaki T, Fukaya M, Shimizu H, Watanabe M (2003) Subtype switching of vesicular glutamate transporters at parallel fibre-Purkinje cell synapses in developing mouse cerebellum. *Eur J Neurosci* 17:2563–2572.
3. Hadjantonakis AK, Gertsenstein M, Ikawa M, Okabe M, Nagy (1998) A generating green fluorescent mice by germline transmission of green fluorescent ES cells. *Mech Dev* 76:79–90.
4. Letellier M, et al. (2007) Reinnervation of late postnatal Purkinje cells by climbing fibers: neosynaptogenesis without transient multi-innervation. *J Neurosci* 27:5373–5383.
5. Konnerth A, Llano I, Armstrong CM (1990) Synaptic currents in cerebellar Purkinje cells. *Proc Natl Acad Sci USA* 87:2662–2665.
6. Fiala JC (2005) Reconstruct: A free editor for serial section microscopy. *J Microsc* 218:52–61.
7. Hashimoto K, Kano M (2003) Functional differentiation of multiple climbing fiber inputs during synapse elimination in the developing cerebellum. *Neuron* 38:785–796.

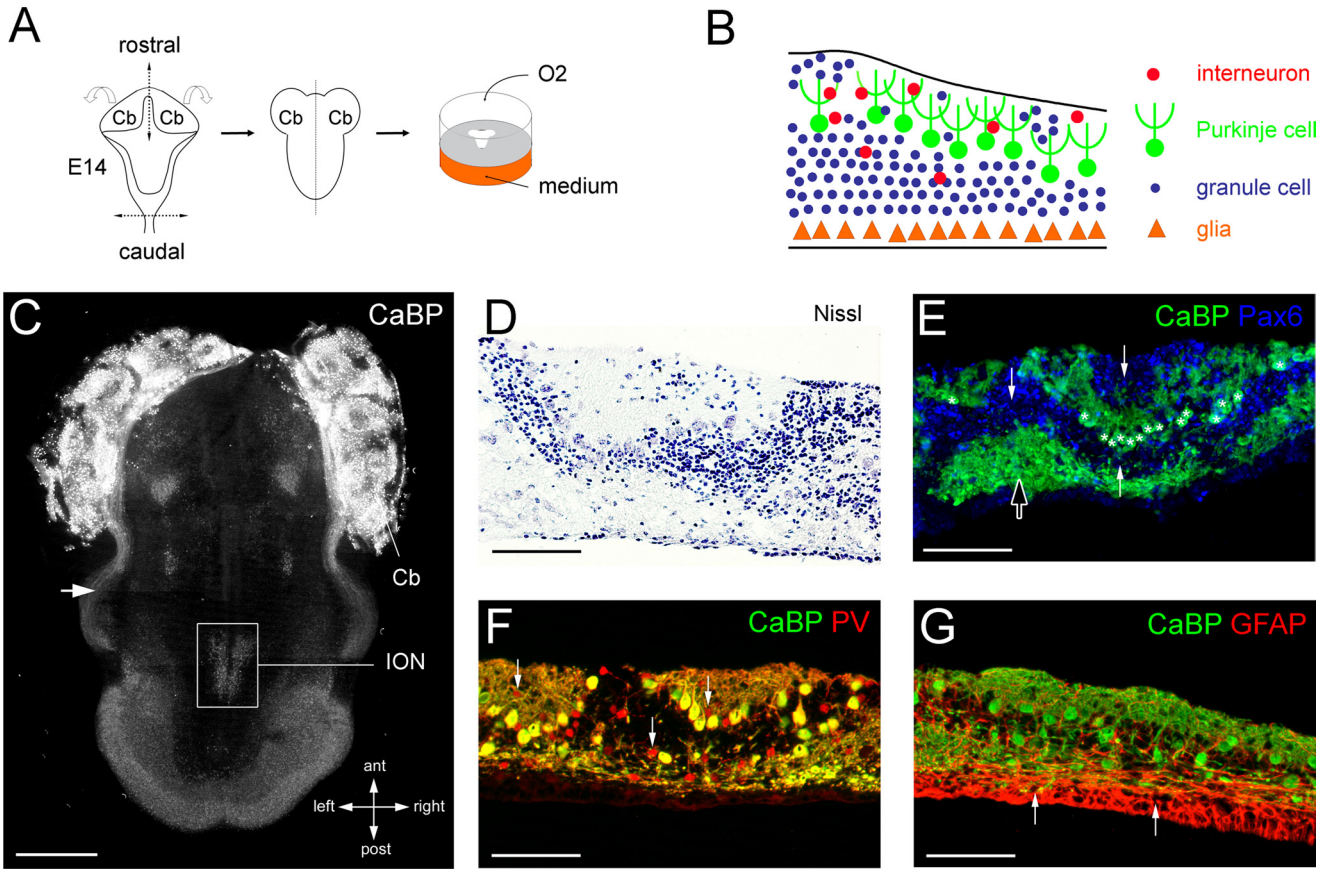

Fig. S1. Cellular organization of the cerebellar system in mature hindbrain explants. (*A*) Procedure for mouse explants cultures at E14, adapted from Chedotal et al. (1). The dashed lines with arrows indicate cuts. Hindbrains containing the cerebellum and the brainstem are opened (thick arrows) and cultured as ''openbooks'' on millicell membranes. (*B*) Schematic cellular organization of the cerebellar system in hindbrain explants. (*C*) Fluorescence micrograph showing a whole explant after 28 DIV, immunolabeled with CaBP antibody. The right and left cerebellar plates (Cb) contain numerous CaBP-positive PCs, which send their axons to a more caudal position, probably corresponding to the vestibular nuclei (arrow). On both sides of the midline, the inferior olivary nucleus (ION) contains CaBP-positive neurons. (*D*) Transverse section stained with cresyl violet showing the laminar organization of cerebellar plates after 25 DIV. (*E–G*) Fluorescence micrograph showing the arrangement of CaBP-positive Purkinje cells (asterisks in *E*) and the distribution of Pax6-positive granule cells (*E*), PV-positive interneurons (*F*), and GFAP-positive glial cells (*G*) in transverse sections from explants at 25 DIV. PC cell bodies are arranged in a pseudomonolayer; they orientate their dendritic tree toward the top of the explant and send their axons to the lower part (*E–G*, black arrow in *E*). Many Pax6-positive GCs are found either below or above the PC layer (*E*, white arrows). PV-positive interneurons are found throughout the thickness of cerebellar plates (*F*, white arrows). GFAP-positive glial cells are found primarily in the lower part of the explant and extend processes throughout the thickness of the cerebellar plate (*G*, white arrows). (Scale bars: *C*, 1 mm; *D–G*, 100 μm.)

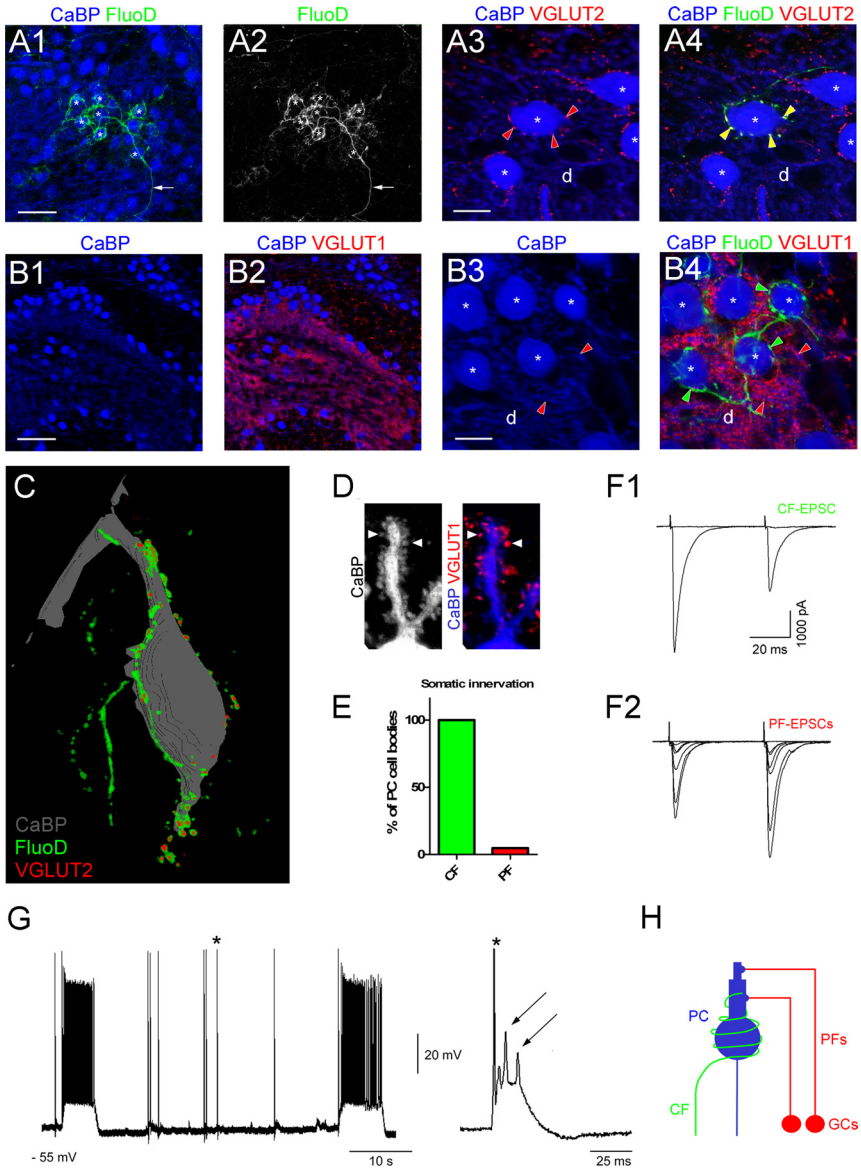

Fig. S2. Mature PCs receive both PF- and CF-synaptic inputs in explants. (*A1–B4*) Confocal sections from whole explants at 25 DIV are showing labeling for CaBP-positive PCs (blue) and anterograde-labeled CFs (green) with additional immunostaining for VGLUT2 (red) (*A3* and *A4*) or VGLUT1 (red) (*B2* and *B4*). Anterograde-labeled CFs surround the cell body of several PCs (asterisks, *A1–A4*) and colocalize with VGLUT2-positive puncta (*A3* and *A4*, red and yellow arrowheads), but not with VGLUT1 puncta (green arrowheads for CF terminals and red arrowheads for PF terminals, *B4*). VGLUT1-positive PF terminals are found contacting PC dendrites (d) (red arrowheads, *B3* and *B4*), whereas VGLUT2-positive terminals are primarily found contacting PC cell bodies (*A3* and *A4*). (*C*) Three-dimensional reconstruction of one PC (gray) innervated by an anterograde-labeled CF (green) expressing VGLUT2 (red). Both the soma and dendritic trunks are innervated by VGLUT2-immunopositive CF terminals. (*D*) Confocal sections from whole explants at 25 DIV showing CaBP dendrites (white or blue) innervated by VGLUT1-positive PF terminals (red) onto spines (arrowheads). (*E*) Histogram showing the percentage of PC cell bodies innervated by VGLUT2-immunopositive CFs filled with the anterograde label fluorodextran (green column) and by VGLUT1-immunopositive PFs (red column). (*F1* and *F2*) Examples of CF-EPSC (*F1*) and PF-EPSC (*F2*) recorded from PCs in an explant at 25 DIV. The PF response displays short-term facilitation in response to a double stimulation and its amplitude increases in a graduated manner as the stimulation intensity increased. The CF response displays short-term depression in response to a double stimulation and its amplitude increases in an all-or-none fashion as the stimulation intensity increased. Holding potentials were −80 mV. (*G*) Spontaneous activity recorded under the current clamp mode in a PC from an explant at 25 DIV. The PC potential membrane displays bistability, regularly switching between a hyperpolarized state and a firing depolarized state. The PC exhibits both spontaneous SSs and typical CSs (asterisks) with regenerative spikelets (arrows). (*H*) Schematic representation of the pattern of innervation of mature PCs by PFs and CFs. (Scale bars: *A1* and *A2*, 50 μm; *B1* and *B2*, 100 μm; *A3* and *A4*, *B3* and *B4*, 20 μm.)

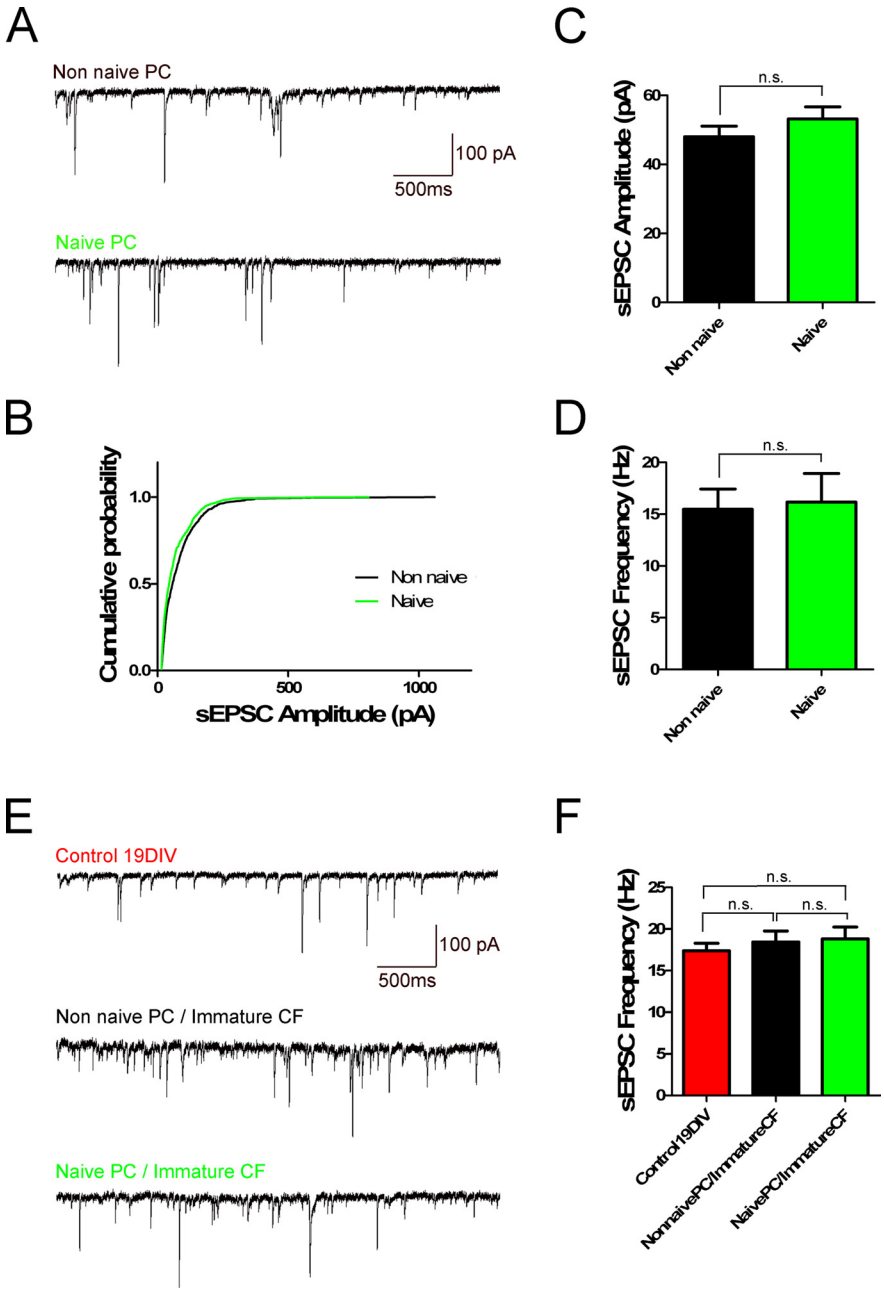

Fig. S3. PF synaptic input is present in cocultures. (*A–D*) Non-naive and naive PCs display similar PF-synaptic input before CF (re)innervation. (*A*) Spontaneous activity recorded under voltage-clamp in non-naive (*Upper*) and naive (*Lower*) PCs. Holding potentials were −80 mV. (*B*) Cumulative distribution of sEPSCs amplitudes from corresponding representative PCs. (*C* and *D*) Histograms showing the mean sEPSC amplitude (*C*) and the mean sEPSC frequency from non-naive PCs (black bar) and naive PCs (green bar). (*E* and *F*) Non-naive and naive PCs during (re)innervation in cocultures receive spontaneous excitatory synaptic input similar to that of normal development. (*E*) Spontaneous activity recorded under voltage-clamp in a control PC at 19 DIV (*Top*), a non-naive PC reinnervated by immature CFs (*Middle*) and a naive PC innervated by immature CFs (*Bottom*). Holding potentials were −80 mV. (*F*) Histogram showing the mean sEPSCs amplitude from the three experimental conditions. Data are expressed as mean ± SEM.

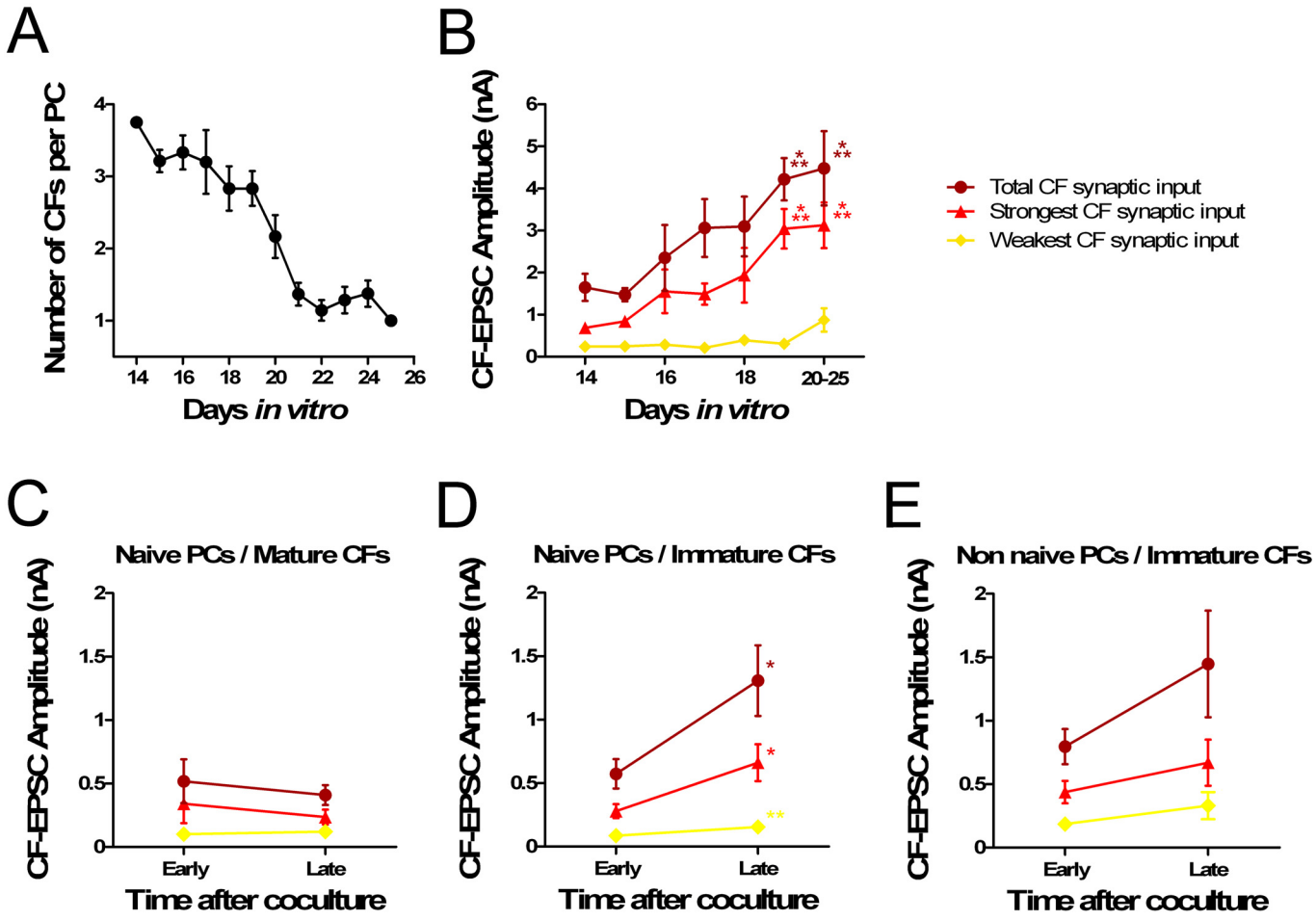

Fig. S4. Maturation of the CF synaptic input during normal development and in cocultures. (*A*) Graph showing the mean number of CF-EPSCs per PC during normal development. (*B*) Graph showing the amplitude of the strongest (red), the weakest (yellow), and the total CF synaptic response (dark red) during normal development. (*C–E*) Graphs showing the amplitude of the strongest (red), the weakest (yellow), and the total CF synaptic response (dark red) during innervation of naive PCs by mature (*C*) or immature (*D*) CFs and during reinnervation of non-naive PCs by immature CFs (*E*). Statistical significance is indicated as follows: *, $0.01 < P < 0.05$; **, $0.001 < P < 0.01$; and ***, $P < 0.001$. Data are expressed as mean ± SEM.

Table S1. Respective roles of the synaptic partners in the control of synaptic competition: A summary of studies in vivo and in vitro

CFs	Experimental paradigm	Initial no. of synaptic CF affluents	Selective synapse elimination and stabilization
Immature CFs			
Immature PCs	Normal development/ early post-lesional reinnervation[1, 2, 3]	Multi-innervation	YES → Mono-innervation (by synaptic competition)
Naive PCs, >21 DIV	Heterochronic cocultures	Multi-innervation	NO
Non-naive PCs, >21 DIV	Heterochronic cocultures	Multi-innervation	NO
Mature CFs			
Immature PCs	Graft experiments[4,5,6]	Multi-innervation	YES → Mono-innervation (by synaptic competition)
Naive PCs, >21 DIV	Isochronic cocultures	Multi-innervation	NO
Non-naive PCs, >21 DIV	Late postnatal reinnervation[4]/ isochronic cocultures	Mono-innervation (without synaptic competition)	X

1. Hashimoto K, Kano M (2003) Functional differentiation of multiple climbing fiber inputs during synapse elimination in the developing cerebellum. *Neuron* 38:785–796.
2. Mariani J, Changeux JP (1981) Ontogenesis of olivocerebellar relationships. I. Studies by intracellular recordings of the multiple innervation of Purkinje cells by climbing fibers in the developing rat cerebellum. *J Neurosci* 1:696–702.
3. Lohof AM, Mariani J, Sherrard RM (2005) Afferent-target interactions during olivocerebellar development: Transcommissural reinnervation indicates interdependence of Purkinje cell maturation and climbing fibre synapse elimination. *Eur J Neurosci* 22:2681–2688.
4. Letellier M, et al. (2007) Reinnervation of late postnatal Purkinje cells by climbing fibers: Neosynaptogenesis without transient multi-innervation. *J Neurosci* 27:5373–5383.
5. Gardette R, Crepel F, Alvarado-Mallart RM, Sotelo C (1990) Fate of grafted embryonic Purkinje cells in the cerebellum of the adult "Purkinje cell degeneration" mutant mouse. II. Development of synaptic responses: An in vitro study. *J Comp Neurol* 295:188–196.
6. Tempia F, Bravin M, Strata P (1996) Postsynaptic currents and short-term synaptic plasticity in Purkinje cells grafted onto an uninjured adult cerebellar cortex. *Eur J Neurosci* 8:2690–2701.